JMEPEG (2023) 32:10834–10842
https://doi.org/10.1007/s11665-023-07908-3

1059-9495/$19.00

TECHNICAL ARTICLE

Comparative Study on Microstructure and Tribological Property of VCN, VCN-Al, and VCN/Al Films

Zhaobing Cai, Jingsheng Mao, Zheng Wang, Wuming Guo, Feihuan Chen, Yinghui Dong, Po Zhang, and Le Gu

Submitted: 24 November 2022 / Revised: 24 December 2022 / Accepted: 13 January 2023 / Published online: 7 February 2023

In this paper, VCN film, VCN-Al composite film and VCN/Al multilayer film were prepared by multi-arc ion plating. The microstructure and tribological properties of these films were studied and analyzed in detail. The results show that the VCN, VCN-Al and VCN/Al films are all mainly composed of VCN phase, and Al phase appears in VCN-Al and VCN/Al films as expected. The sp^2 C-C and sp^3 C-C can be detected in these films, but they play a limited role in the improvement of the tribological property. Owing to the relatively low nano-hardness of metal Al, and a relatively high friction coefficient of formed Al-Oxides (Al_2O_3), the Al-containing VCN films have poor wear resistance compared to the VCN film. The multilayer structure of VCN/Al film with the lowest nano-hardness improves the wear resistance to some extent, leading to the wear rate being slightly lower than that of VCN-Al film. However, the wear mechanism of VCN, VCN-Al and VCN/Al films can all be considered adhesive wear and oxidative wear.

Keywords Al-oxides, tribological property, VCN-Al composite, VCN/Al multilayer, wear mechanism

1. Introduction

In the past decades, hard films such as TiN, CrN, W_2N and VN have been widely used and studied in aerospace, petroleum, metallurgy and machinery industries due to their good hardness, wear resistance, high-temperature resistance and corrosion-resistance (Ref 1-5). Because VN is easy to react with O_2 during the friction process to generate V-containing oxides (like V_2O_5) that effectively reduce the friction coefficient, the VN films have been regarded as ideal substitutes for the more commercial TiN and CrN, to solve the problem of friction and wear; thereby, they have been extensively studied (Ref 6-9).

However, when VN films with high self-lubrication capability are subjected to some extreme environments, such as high humidity and high temperature, the traditional solid lubricants fail and their hardness and oxidation resistance rapidly decrease, which greatly limits their application (Ref 10). Up to now, studies have shown that the doping of C can effectively improve the tribological properties of VN-based films (Ref 11-14). For example, Cai et al. (Ref 12) found that doping C improved the mechanical and tribological properties of VN films and reduced surface roughness and residual stress. Cai et al. (Ref 13) also found that VC phase and sp^2 hybrid carbon occurred in the C-doped VN film, which plays a key role in improving the hardness of the film and reducing the friction coefficient, respectively. Mu et al. (Ref 14) demonstrated that at different temperatures even at 700 °C, the friction coefficient and wear rate of the VCN film were lower than those of the VN film. Subsequently, to further improve the comprehensive properties of VCN films, researchers have made many attempts to improve the properties of VCN films, mainly including single-component or multi-component doping and multilayer structure design. Like, VAlCN (Ref 15), VAlCN/VN-Ag (Ref 16), VCN-Ag (Ref 17, 18), VCN-Cu (Ref 19) and TiAlCN/VCN (Ref 20). It was found that Al incorporation could improve the hardness and oxidation resistance of VCN films. For example, Wang et al. (Ref 15) designed V-Al-C-N nanocomposite film. The results indicate that under 10N, the wear rate of the film was lower ($< 1.5 \times 10^{-16}$ $m^3 \cdot N^{-1} \cdot m^{-1}$) and toughness is significantly improved. In addition, multilayer films are proved to be a promising method, which can inhibit the growth of columnar crystals and the initiation and propagation of cracks, thus improving the comprehensive properties (Ref 21, 22). Cai et al. (Ref 16) also found that the multilayer VAlCN/VN-Ag film has a higher hardness ($\sim$ 27 GPa) and elastic modulus ($\sim$ 370 GPa) than the

Zhaobing Cai, Key Laboratory of Metallurgical Equipment and Control Technology, Ministry of Education, Wuhan University of Science and Technology, Wuhan 430081, China; and Precision Manufacturing Institute, Wuhan University of Science and Technology, Wuhan 430081, China; **Jingsheng Mao** and **Po Zhang**, Key Laboratory of Metallurgical Equipment and Control Technology, Ministry of Education, Wuhan University of Science and Technology, Wuhan 430081, China; **Zheng Wang** and **Le Gu**, Key Laboratory of Metallurgical Equipment and Control Technology, Ministry of Education, Wuhan University of Science and Technology, Wuhan 430081, China; and Hubei Key Laboratory of Mechanical Transmission and Manufacturing Engineering, Wuhan University of Science and Technology, Wuhan 430081, China; **Wuming Guo**, Key Laboratory of Marine Materials and Related Technologies, Ningbo Institute of Materials Technology and Engineering, Chinese Academy of Sciences, Ningbo 315201, China; **Feihuan Chen**, Hubei Key Laboratory of Mechanical Transmission and Manufacturing Engineering, Wuhan University of Science and Technology, Wuhan 430081, China; and Key Laboratory of Marine Materials and Related Technologies, Ningbo Institute of Materials Technology and Engineering, Chinese Academy of Sciences, Ningbo 315201, China; and **Yinghui Dong**, Precision Manufacturing Institute, Wuhan University of Science and Technology, Wuhan 430081, China. Contact e-mails: caizhaobing@wust.edu.cn and hitribology@163.com.

VAlCN-Ag film, and the friction coefficient ($\sim$ 0.25) and wear rate ($\sim 3.7 \times 10^{-5}$ $m^3 \cdot N^{-1} \cdot m^{-1}$) of VAlCN/VN-Ag multilayer film are lower. However, a fact must be recognized that soft metal Al in the present form of metallic phase will decrease the hardness of films. So it is important to clarify the competition between doping Al and multilayer structure design based on the research of VCN film, which can be used as a guide for future film design and industrial application (Ref 23).

In this work, VCN, VCN-Al composite and VCN/Al multilayer films are designed and prepared. The microstructure and tribological behavior of these films are studied in detail, and the relationship between soft metal Al doping and multilayer structure design is explored and analyzed.

2. Experimental Details

The VCN film, VCN-Al composite film and VCN/Al multiple-layer film (denoted as VCN, VCN-Al and VCN/Al film, respectively, in the following text) were deposited on 316L stainless steel and silicon wafer substrates using the Hauzer Flexicoat 850-type multi-arc ion plating system with pure V and Al targets (purity > 99.5 wt.%). The specific preparation process of VCN film and VCN-Al film can be found in our previous literature (Ref 12, 13) with a little bit of difference in the main preparation parameters: Ar gas flow of 150 sccm, N_2 gas flow of 800 sccm, C_2H_2 gas flow of 40 sccm, V target current of 65 A, Al target current of 40 A, substrate bias of − 75 V, substrate temperature of 450 °C and deposition time of 4 h. However, the VCN/Al film was also prepared with the same preparation parameters according to the following multiple-layer design: VCN layer (5 min)/Al (2 min)/VCN layer (5 min)./VCN layer (5 min)/Al (2 min)/VCN layer (5 min).

The friction and wear tests of the VCN, VCN-Al and VCN/Al films were conducted at least three times on a ball-on-disk HVTRB tribometer (CSM instruments) against a 6-mm-sized Al_2O_3 ball at room temperature with the test parameters as follows: The normal load was 5 N, the radius of the wear tracks was 5 mm, the rotation speed of 200 rpm and the sliding distance of 200 m. After the friction and wear test, the height and width, as well as the wear area of the wear scars, were obtained by an α-Step IQ profilometer. The specific wear-rate of the films was calculated by the equation: specific wear-rate = $S \cdot 2\pi r/(F \cdot L)$ (S is the cross-sectional area of the wear scar, r is the radius of the wear scar, F is the normal load, and L is the sliding distance).

The phase composition of films was characterized by a BRUKER D8 Advance x-ray diffractometer (XRD) with Cu radiation at the 2θ range of 20° $\sim$ 90°. The surface and cross section morphologies as well as wear scars of films were observed by an EVO 18-type big-cavity scanning electron microscope (SEM) equipped with energy-dispersive x-ray spectroscopy (EDS). Further, the cross section morphology of VCN/Al film was observed by a Talos F200x transmission electron microscopy (TEM). The Renishaw inVia Reflex-type Raman spectroscopy was used to analyze the characteristic peaks of C atomic crystal in these films at the Raman shifts of 620 cm^{-1} $\sim$ 2300 cm^{-1}. The hardness and elastic modulus of films were measured by an MTS Nano Indenter G200 system equipped with a Berkovich indenter using continuous stiffness method with a maximum indentation depth of 1000 nm, and six indentation measurement values were taken from different areas of each sample to obtain the average value.

3. Results and Discussion

Figure 1 shows the XRD patterns of VCN, VCN-Al and VCN/Al films. As can be seen, there are five diffraction peaks at 2θ = 37.44°, 43.39°, 63.23°, 76.11° and 79.50°, corresponding to (1 1 1), (2 0 0), (2 2 0), (3 1 1) and (2 2 2) crystal planes of VN phase [JCPDF #78-1315] and VC phase [JCPDF #73-0476] (Ref 1). The diffraction peak of pure Al can be observed in the XRD pattern of VCN/Al film as expected (see the partial enlargements of 2θ = 36° $\sim$ 39° and 42° $\sim$ 45°). In addition, the Al phase seems to appear in the XRD pattern of VCN-Al film with relatively low peak strength, indicating that a small amount of Al phase is dispersed in the VCN-Al film. However, compared to VCN film, the peak position of the VN or VC phase in VCN-Al film shifts toward the right, which shows that the Al is solidly dissolved in the VN or VC lattice, but does not react with N to form the AlN phase.

The surface and cross section morphologies of the VCN, VCN-Al and VCN/Al films are displayed in Fig. 2. From the surface morphologies of (Fig. 2a, b and c), many spherical macro-particles and micro-cavities can be seen, which belongs to the technical feature of multi-arc ion plating (Ref 24, 25), and there are more micro-particles on the surface morphology of VCN-Al and VCN/Al film than that of VCN film, which may be attributed to that the melting point of metal Al is much lower than that of metal V, leading to the easy formation of Al large drops. Table 1 gives the surface elemental composition of the VCN, VCN-Al and VCN/Al films. It can be seen that there are so many contents of Al element on the surface of the VCN-Al and VCN/Al films, which proves laterally that metal Al is much easier to form the large drops than metal V during multi-arc ion plating. As shown in the cross-sectional morphologies in Fig. 2(d), (e) and (f), the structure of VCN, VCN-Al and VCN/Al films tends to be featureless with no big difference. Based on Fig. 2(d), (e) and (f), the cross section element composition and thickness of VCN, VCN-Al and VCN/Al films are shown in Table 2. To our knowledge, the ratio of (C + N)/V has to do with the structure of VCN films. That is, when the ratio is above 1.2, VCN film will exhibit the typical columnar crystalline structure, while the ratio is below 1, it will become the disordered and featureless structure (Ref 13, 14). Thus, it can be concluded that the ratio of (C + N)/V of VCN, VCN-Al and VCN/Al films is all < 1, so these films display disordered and featureless structures. Moreover, the thickness of VCN, VCN-Al and VCN/Al films is 4.34, 12.20 and 6.67 um, respectively, which can be inferred that the Al may promote the deposition rate of VCN films.

Figure 3 reveals the TEM micrograph and element mappings of VCN/Al film. From the TEM micrograph, the VCN/Al film shows the typical multilayer structure as expected. According to the element mappings, the thick layer is mainly composed of V, C and N elements, corresponding to VCN film, while the thin layer is primarily composed of Al element, corresponding to Al film. By measurement, the VCN film mono-layer is $\sim$ 150 nm, but the Al mono-layer is below 10 nm.

Raman was used to further study the phase composition of VCN, VCN-Al and VCN/Al films displayed in Fig. 4, showing

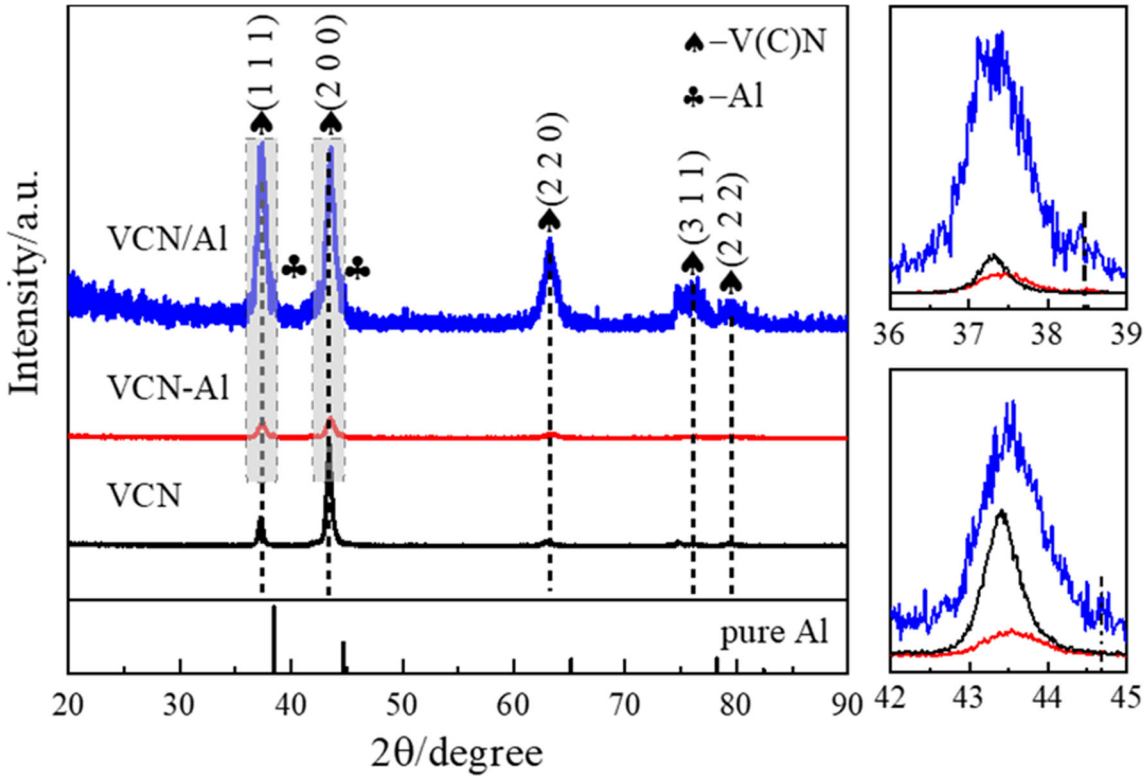

Fig. 1 XRD patterns of VCN, VCN-Al and VCN/Al films

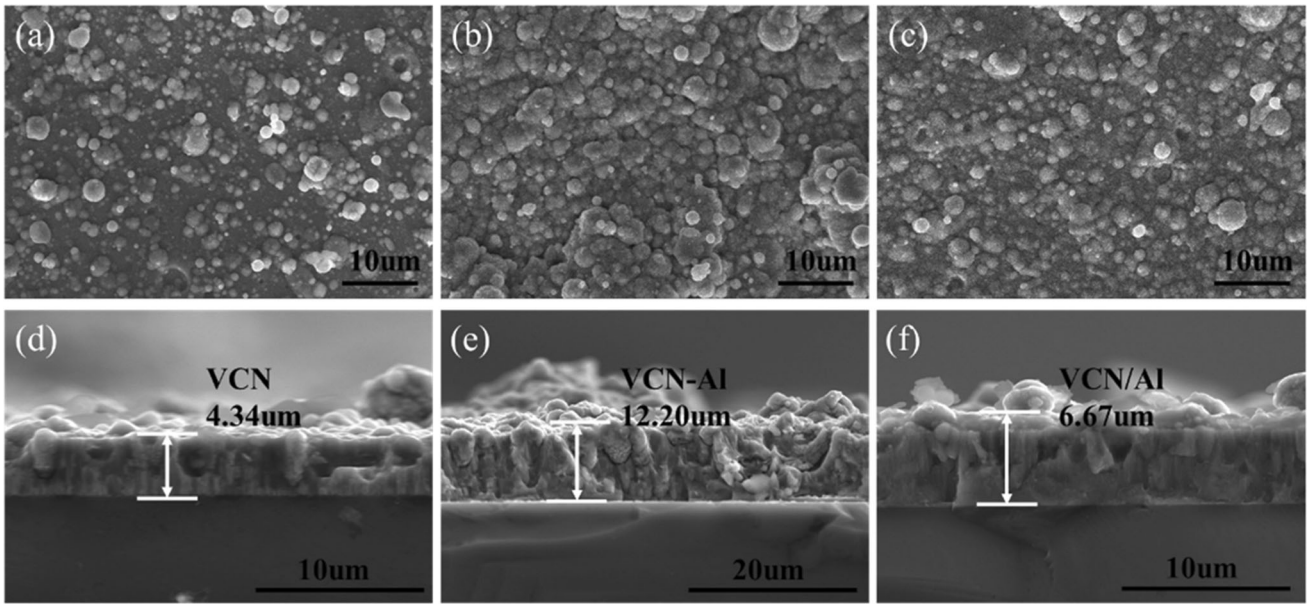

Fig. 2 Surface and cross section SEM images of different films: (a) (d) VCN, (b) (e) VCN-Al and (c) (f) VCN/Al

that the Raman spectra of VCN, VCN-Al and VCN/Al films are roughly the same. By analysis, there are two relatively weak peaks at $\sim$ 700 and $\sim$ 800 cm^{-1}, and combined with the phase analysis of XRD patterns (Fig. 1), these characteristic peaks should be assigned to the VN phase, which is in keeping with the previous literature (Ref 12, 19). However, peaks at $\sim$ 1381 cm^{-1} of D peak (diamond, sp^3 C-C) and $\sim$ 1580 cm^{-1} of G peak (graphite, sp^2 C-C) can be clearly observed. The Raman shifts at 1000^{-1} – 1800 cm^{-1} of VCN, VCN-Al and VCN/Al films are presented to use to the ratio of I_D/I_G. By fitted and calculation, the I_D/I_G ratios of VCN, VCN-Al and VCN/Al films are 3.24, 1.92 and 2.08, respectively. In general, different proportions of sp^3 C-C and sp^2 C-C can significantly affect the mechanical and tribological properties of nitride films (Ref 13, 19, 26). The diamond-like structure of sp^3 C-C will improve the hardness and wear resistance of films, while the graphite-like structure of sp^2 C-C will reduce the friction coefficient of films. Thus, the VCN film may have a good wear resistance but a high

friction coefficient, and the Al-containing VCN films will have a relatively poor wear resistance but a low friction coefficient. The nano-hardness (H) and elastic modulus (E) as well as the ratio of H/E and H^3/E^2 of VCN, VCN-Al and VCN/Al films by nano-indentation are displayed in Fig. 5. From Fig. 5(a), the nano-hardness of VCN, VCN-Al and VCN/Al films is 31.98 ± 2.55, 15.91 ± 1.96 and 3.91 ± 0.31 Gpa, respectively, and the elastic modulus of VCN, VCN-Al and VCN/Al films is 540.8 ± 24.39, 213.09 ± 21.02 and 31.76 ± 2.67 GPa, respectively, indicating that Al-containing VCN films (VCN-Al and VCN/Al films) have a decreased nano-hardness and elastic modulus because of the low hardness of soft metal Al, which has been demonstrated in other hard films containing soft metals (Ref 18, 27). However, the VCN-Al film has more Al content than the VCN/Al film (shown in Table 2), and the nano-hardness of VCN-Al film is higher than that of VCN/Al film, which is due to the strengthening effect of the solid solution by that some of the Al are solidly dissolved in the VN or VC lattice in the VCN-Al film (shown in Fig. 1). Figure 5(b) shows the H/E and H^3/E^2 ratios of VCN, VCN-Al and VCN/Al films. It is well known that the ratios of H/E and H^3/E^2 are concerned about the durability and plastic deformation resistance of the films, and the higher H/E and H^3/E^2 will have a better tribological property. From Fig. 5(b), the H^3/E^2 of these films is ranked as VCN > VCN-Al > VCN/Al, while the H/E is ranked as VCN/Al > VCN-Al > VCN. Therefore, the contrast of tribological behavior of VCN, VCN-Al and VCN/Al films is unpredictable. Figure 6 shows the tribological behavior of VCN, VCN-Al and VCN/Al films with the Al_3O_2 grinding ball at room temperature. As can be seen in Fig. 6(a), the friction coefficient of VCN-Al film rapidly reaches the stable wear stage (about 100 s at the beginning of the test) until the end of the friction and wear test, while the VCN and VCN/Al film have a larger fluctuation (about 200 s $\sim$ 400 s) at the initial run-in and wear stage. It may be attributed to the surface of VCN-Al film having a lot of large drops of Al metal, which is easy to be oxidized to form Al_2O_3 wear debris, in turn, the Al_2O_3 wear debris sticks to the Al_3O_2 grinding ball, to form a stable friction state of the VCN-Al film quickly. According to Fig. 6(a), the average friction coefficients of VCN, VCN-Al and VCN/Al films are 0.51 ± 0.04, 0.58 ± 0.04 and 0.68 ± 0.04, respectively, displayed in Fig. 6(c). Figure 6(b) shows the depth and width of wear scar of VCN, VCN-Al and VCN/Al films. It can be seen that among these films, the depth and width of the wear scar of VCN film are the smallest, while the width and depth of VCN-Al film and VCN/Al film are almost the same and larger. Based on Fig. 6(b), the wear volume of VCN, VCN-Al and VCN/Al films can be obtained, and the calculated wear rate of VCN, VCN-Al and VCN/Al films is shown in Fig. 6(c), which are $(2.41 \pm 0.13) \times 10^{-14}$ $m^3 \cdot N^{-1} \cdot m^{-1}$, $(10.35 \pm 0.35) \times 10^{-14}$ $m^3 \cdot N^{-1} \cdot m^{-1}$ and $(10.2 \pm 0.42) \times 10^{-14}$ $m^3 \cdot N^{-1} \cdot m^{-1}$, respectively, indicating

Table 1 Surface element composition of VCN, VCN-Al and VCN/Al films

	Element composition			
At.%	C	N	V	Al
VCN	10.77	15.65	73.58	…
VCN-Al	9.39	19.29	4.51	66.81
VCN/Al	9.87	17.78	1.98	70.37

Table 2 Cross section element composition and thickness of VCN, VCN-Al and VCN/Al films

	Element composition				Thickness
At.%	C	N	V	Al	
VCN	12.54	6.51	80.95	…	4.34
VCN-Al	2.54	2.44	89.58	5.44	12.20
VCN/Al	12.41	13.42	71.28	2.89	6.67

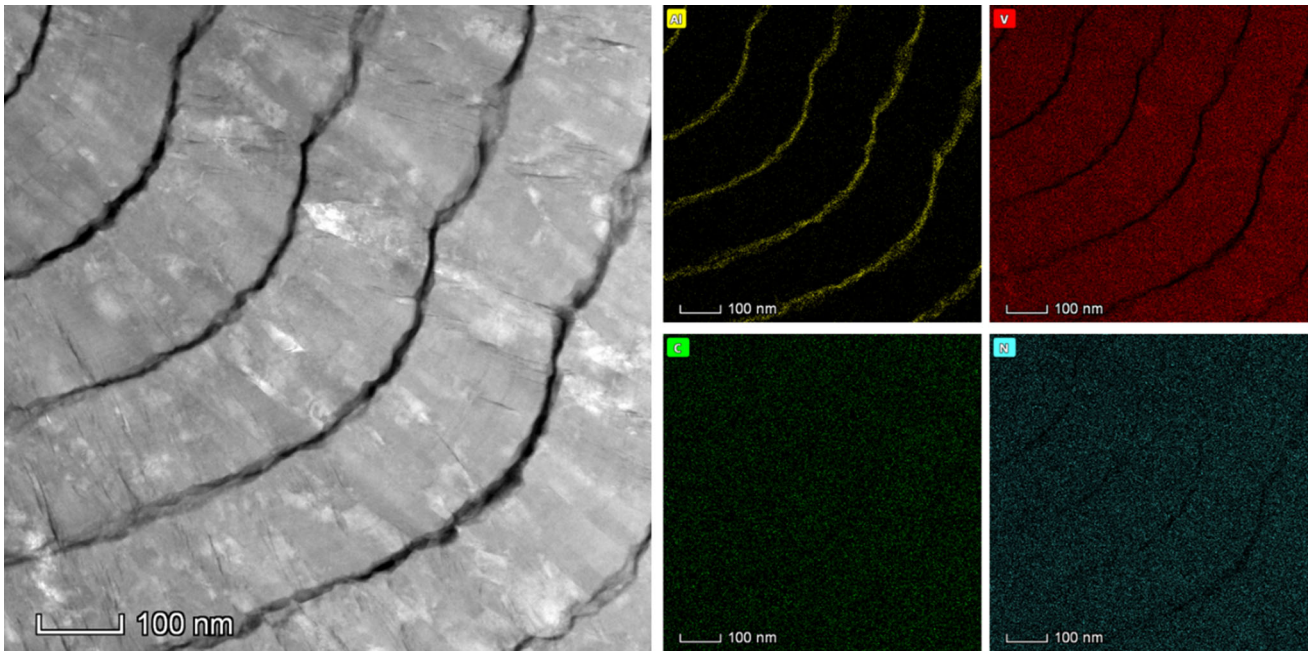

Fig. 3 TEM micrograph and element mappings of VCN/Al film

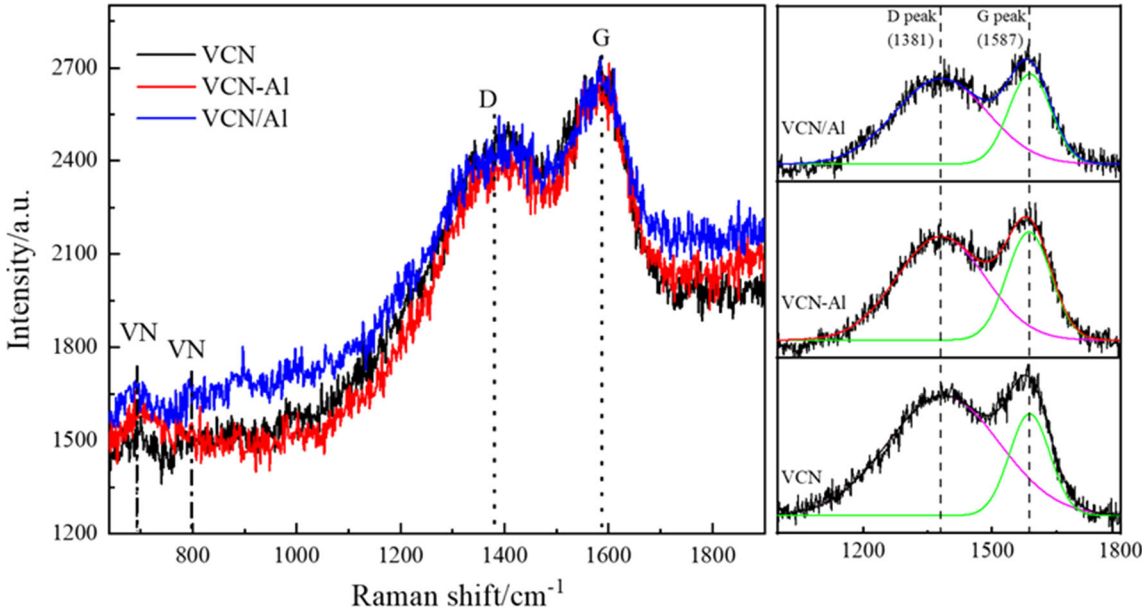

Fig. 4 Raman spectra of VCN, VCN-Al and VCN/Al films (the right view are the fitted curves at Raman shift of 1000-1800 cm^{-1})

that the wear resistance of the VCN film is the best, while the wear resistance of VCN-Al and VCN/Al film is relatively poor.

Figure 7 shows the SEM micrographs of the worn surfaces of VCN, VCN-Al and VCN/Al films with the corresponding Al_3O_2 grinding ball. As shown in Fig. 7(a), (b) and (c), the worn surface of VCN film is relatively smooth and the width of the wear scar is narrow, further proving that compared to VCN-Al and VCN/Al films, the VCN film has the best wear resistance under the same friction condition. In addition, the wear width of VCN-Al film and VCN/Al film is about the same, and the wear degree of these two films is about the same with some flake debris caused by plastic deformation in some areas. The tables in the top right corner of Fig. 7a, b and c give the EDS element composition in the wear scar of VCN, VCN-Al and VCN/Al films, indicating the appearance of oxidation. As expected, the oxide in the wear scar of VCN is V-oxides, while that in the wear scar of VCN-Al and VCN/Al films are V-oxides and Al-oxides. Thus, the wear mechanism of VCN, VCN-Al and VCN/Al films can all be considered adhesive wear and oxidative wear. Figure 7(d), (e) and (f) shows the EDS results of transferred film bounding to the Al_2O_3 grinding ball, confirming the formation of Al-oxides (Al_2O_3), and the formation content of Al_2O_3 in VCN/Al film seems to be higher than that in VCN-Al film.

Generally speaking, the hardness is proportional to the wear resistance according to Archard's law (Ref 12). Compared to VCN film, the Al-containing VCN films have a relatively poor wear resistance (Fig. 6c) owing to the relatively low nano-hardness (Fig. 5a). However, the nano-hardness of VCN/Al film is the lowest, but its wear rate is slightly lower than that of VCN-Al film, which may be because the multilayer structure of VCN/Al film helps to offset hardness and reduce friction and can make it have higher strength and toughness, resulting in the improvement of the wear resistance (Ref 21, 22, 28). Moreover, according to the Raman analysis (Fig. 4), the VCN film may have a high friction coefficient, and the Al-containing VCN films will have a relatively low friction coefficient. But Fig. 6(a) displays the opposite result. There are two reasons to explain it: (1) The VCN, VCN-Al and VCN/Al films are all mainly composed of the VCN phase with very little amorphous C phase. So the positive effect of sp^2 C-C is very limited. (2) For Al-containing VCN films, Al_2O_3 appears during the friction and wear (Fig. 7). However, Al_2O_3 oxide with low ionic potential will have a high friction coefficient (Ref 29). As for that, the friction coefficient of VCN/Al film is higher than that of VCN-Al film, which may be due to the larger amount of formed Al_2O_3 and the relatively small I_D/I_G ratio in VCN/Al film (Fig. 7).

By comparison, the negative influence of Al layer (mainly reflected in the great decrease in micro-hardness of film) and the positive influence of multilayer design (leading to the improvement of the flexibility and bearing capacity of film)

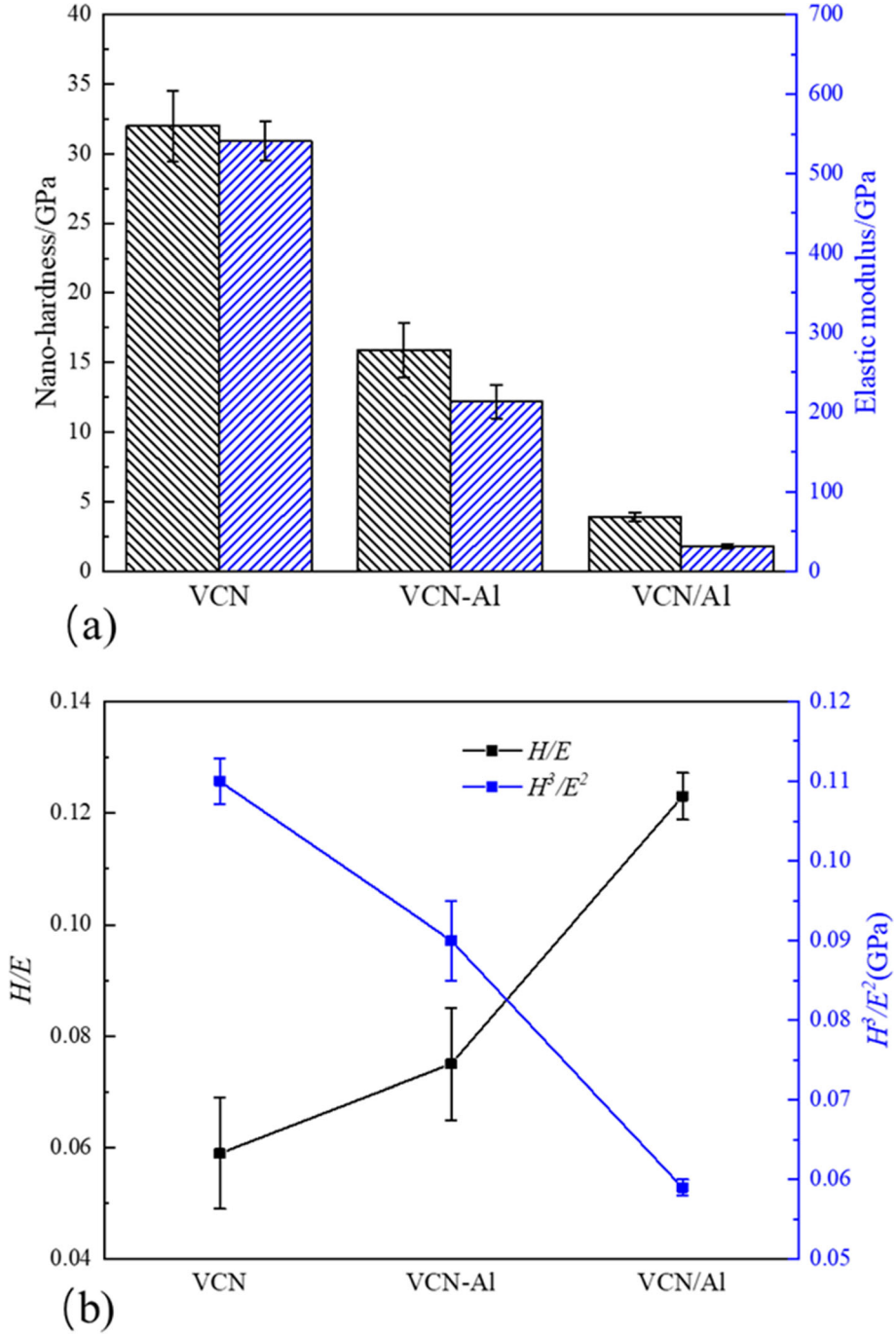

Fig. 5 Nano-hardness and elastic modulus (a) and the ratio of H/E and H^3/E^2 (b) of VCN, VCN-Al and VCN/Al films

display a significant competitive relationship for VCN/Al multiple-layer film. Theoretically speaking, the thickness of Al mono-layer and modulation period of multilayer structure will have a great effect on its performance of VCN/Al multiple-layer film. In future, the study focus is going to be the thickness matching of Al mono-layer and multilayer structure by the control of film deposition parameters.

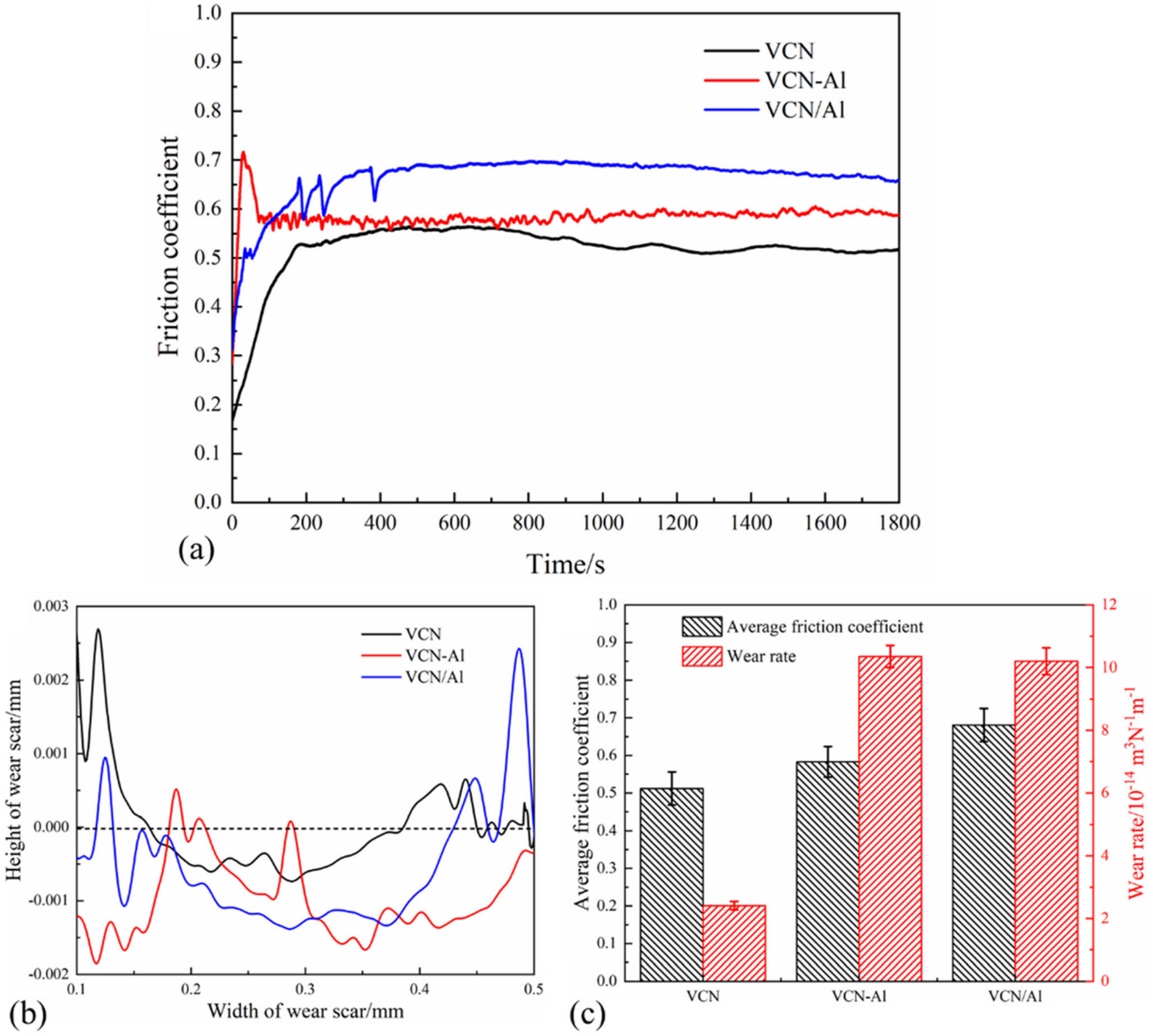

Fig. 6 Tribological behavior of VCN, VCN-Al and VCN/Al films: (a) friction coefficient vs. time, (b) height and width of wear scars and (c) average friction coefficient and wear rate

4. Conclusions

VCN, VCN-Al and VCN/Al films were deposited on 316L stainless steel substrate by a multi-arc ion plating technique. The microstructure and tribological properties of these films were studied. The VCN, VCN-Al and VCN/Al films are all mainly composed of the VCN phase with a certain amount of amorphous C. Al phase appearing in VCN-Al and VCN/Al films is as expected. Compared to the VCN film, the Al-containing VCN films have poor wear resistance owing to the relatively low nano-hardness, and a relatively high friction coefficient due to the formation of Al_2O_3. The multilayer structure of VCN/Al film with the lowest nano-hardness improves the wear resistance to some extent, leading to the wear rate being slightly lower than that of VCN-Al film. However, the wear mechanism of VCN, VCN-Al and VCN/Al films can all be considered adhesive wear and oxidative wear.

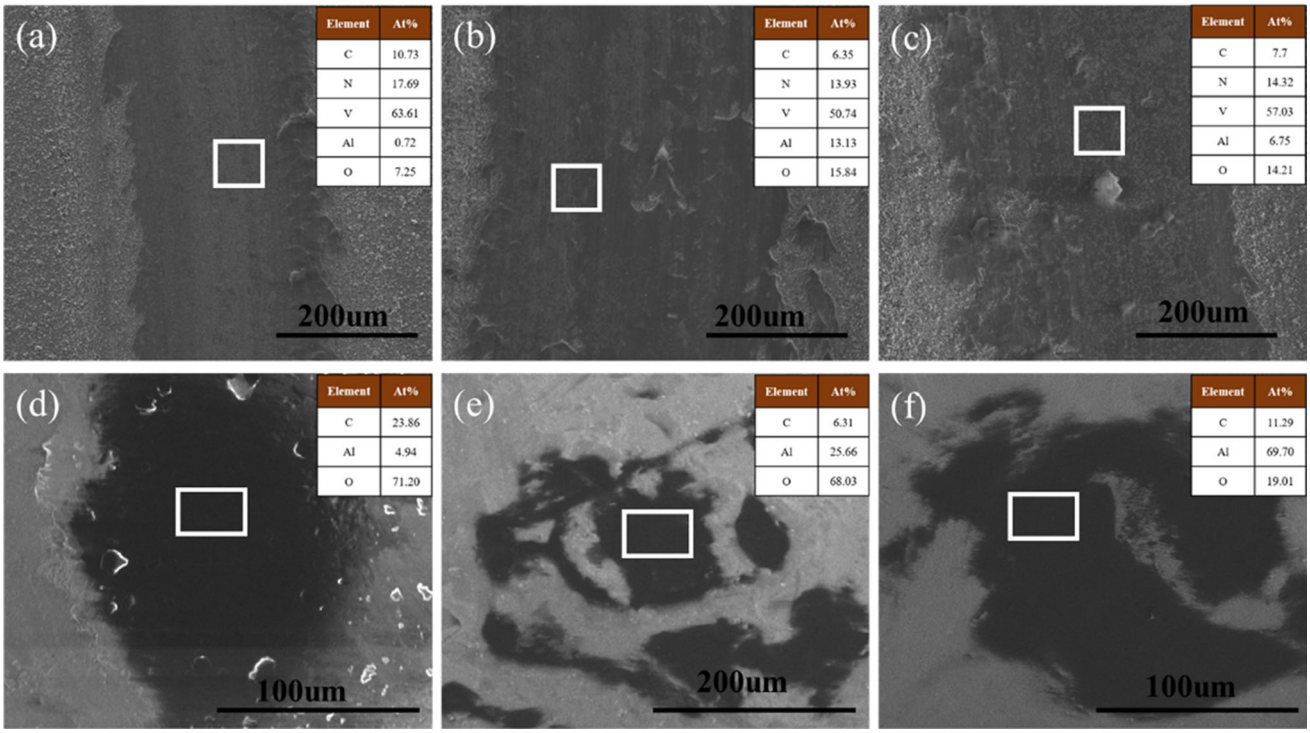

Fig. 7 SEM micrographs of worn surfaces of VCN, VCN-Al and VCN/Al films with the corresponding Al_3O_2 grinding ball: (a) (d) VCN, (b) (e) VCN-Al and (c) (f) VCN/Al

Acknowledgments

The authors gratefully acknowledge the financial support from the National Natural Science Foundation of China (Grant Nos. 51905524 and 52105204).

References

1. C.S. Kumar, S.K. Patel, and F. Fernandes, Performance of Al_2O_3/TiC Mixed Ceramic Inserts Coated with TiAlSiN, WC/C and DLC Thin Solid Films During Hard Turning of AISI 52100 Steel, *J. Mater. Res. Technol.*, 2022, **19**, p 3380–3393
2. C. Pallier, P. Djemia, D. Fournier, L. Belliard et al., Thermal, Electrical, and Mechanical Properties of Hard Nitrogen-Alloyed Cr Thin Films Deposited by Magnetron Sputtering, *Surf. Coat. Technol.*, 2022, **441**, p 128575
3. J.C. Caicedoa, G. Zambrano, and W. Aperador, Mechanical and Electrochemical Characterization of Vanadium Nitride (VN) Thin Films, *Appl. Surf. Sci.*, 2011, **258**, p 312–320
4. H. Ju, N. Ding, J. Xu, L. Yu, Y. Geng, F. Ahmed, B. Zuo, and L. Shao, The Influence of Crystal Structure and the Enhancement of Mechanical and Frictional Properties of Titanium Nitride Film by Addition of Ruthenium, *Appl. Surf. Sci.*, 2019, **489**, p 247–254
5. J.B. Wang, M.Q. Cui, D.C. Wang, Y. Liu, J.Z. Cai, and Z.Q.C.Q. Gu, Integration of Superhydrophobicity and High Durability in Super-Rough Hard Thin Films, *Ceram Int.*, 2021, **47**, p 23653–23658
6. R. Franz and C. Mitterer, Vanadium Containing Self-Adaptive Low-Friction Hard Coatings for High-Temperature Applications: a Review, *Surf. Coat. Technol.*, 2013, **228**, p 1–13
7. H. Torres, M.R. Ripoll, and B. Prakash, Tribological Behaviour of Self-Lubricating Materials at High Temperatures, *Int. Mater. Rev.*, 2018, **63**, p 309–340
8. R. Wang, H.Q. Li, R.S. Li, H.J. Mei, C.W. Zou, T.F. Zhang, Q.M. Wang, and K.H. Kim, Thermostability, Oxidation, and High-Temperature Tribological Properties of Nano-Multilayered AlCrSiN/VN Coatings, *Ceram Int.*, 2022, **48**, p 11915–11923
9. Z.B. Cai, Y. Wu, and J.B. Pu, High-Temperature Friction and Wear Behavior of Varying-C VN Films, *J. Mater. Eng. Perform.*, 2021, **30**, p 2057–2065
10. Y. Qiu, S. Zhang, B. Li, Y. Wang, J.W. Lee, and F. Li, Improvement of Tribological Performance of CrN Coating via Multi-Layering with VN, *Surf. Coat. Technol.*, 2013, **231**, p 357–363
11. S. Calderon Velasco, A. Cavaleiro, and S. Carvalho, Functional Properties of Ceramic-Ag Nanocomposite Coatings Produced by Magnetron Sputtering, *Prog. Mater. Sci.*, 2016, **84**, p 158–191
12. Z.B. Cai, J.B. Pu, L.P. Wang, and Q.J. Xue, Synthesis of a New Orthorhombic form of Diamond in Varying-C VN Films: Microstructure, Mechanical and Tribological Properties, *Appl. Surf. Sci.*, 2019, **481**, p 767–776
13. Q. Cai, S.X. Li, J.B. Pu, Z.B. Cai, X. Lu, Q.F. Cui, and L.P. Wang, Effect of Multi- Component Doping On The Structure And Tribological Properties of VN-Based Coat-Ings, *J. Alloy Compd.*, 2019, **806**, p 566–574
14. Y. Mu, M. Liu, and Y. Zhao, Carbon Doping to Improve the High Temperature Tribological Properties of VN Coating, *Tribol. Int.*, 2016, **97**, p 327–336
15. Z.Y. Wang, X.W. Li, X. Wang, S. Cai, P.L. Ke, and A.Y. Wang, Hard Yet Tough V-Al-C-N Nanocomposite Coatings: Microstructure, Mechanical and Tribological Properties, *Surf. Coat. Technol.*, 2016, **304**, p 553–559
16. Q. Cai, X.B. Bai, and J.B.P. Pu, Adaptive VAlCN-Ag Composite and VAlCN/VN-Ag Multilayer Coatings Intended for Applications at Elevated Temperature, *J. Mater. Sci.*, 2022, **57**, p 8113–8126
17. D. Yu, L. Yu and I. Asempah, Microstructure, Mechanical and Tribological Properties of VCN-Ag Composite Films by Reactive Magnetron Sputtering, *Surf. Coat. Technol.*, 2020, **399**, p 126167
18. A.V. Bondarev, M. Golizadeh, N.V. Shvyndina, I.V. Shchetinin, and D.V. Shtansky, Microstructure, Mechanical, and Tribological Properties of Ag-Free and Ag-Doped VCN Coatings, *Surf. Coat. Technol.*, 2017, **331**, p 77–84
19. Z.B. Cai, R. Chen, W.Z. Wang, J.G. Qian, W.M. Guo, and J.B. Pu, Microstructure and Tribological Properties of Cu-Doped VCN Films: The Role of Cu, *Appl. Surf. Sci.*, 2020, **510**, p 145509
20. L. Quanshun, S. Christian, and P.E. Arutian, Structure and Wear Mechanisms of Nanostructured TiAlCN/VCN Multilayer Coatings, *Plasma Process. Polym.*, 2007, **4**, p 916–920

21. H. Zhang, Z. Li, W. He, B. Liao, G. He, X. Cao, and Y. Li, Damage Evolution and Mechanism of TiN/Ti Multilayer Coatings in Sand Erosion Condition, *Surf. Coat. Technol.*, 2018, **353**, p 210–220
22. G. Pradhaban, P. Kuppusami, D. Ramachandran, K. Viswanathan, and R. Ramaseshan, Nanomechanical Properties of TiN/ZrN Multilayers Prepared by Pulsed Laser Deposition, *Mater. Today Proceed.*, 2016, **3**, p 1627–1632
23. J. Rao, A. Sharma, and T. Rose, Titanium Aluminium Nitride and Titanium Boride Multilayer Coatings Designed to Combat Tool Wear, *Coatings*, 2018, **8**, p 1–12
24. R. Boxman, Macroparticle Contamination in Cathodic Arc Coatings: Generation, Transport and Control, *Surf. Coat. Technol.*, 1992, **52**, p 39–50
25. B. Gao, X.Y. Du, Y.H. Li, S.H. Wei, X.D. Zhu, and Z.X. Song, Effect of deposition Tem- Perature on Hydrophobic CrN/AlTiN Nanolaminate Composites Deposited by Multi- Arc-Ion Plating, *J. Alloy Compd.*, 2019, **797**, p 1–9
26. J.G. Qian, S.X. Li, J.B. Pu, Z.B. Cai, H.X. Wang, Q. Cai, and P.F. Ju, Effect of Heat Treatment on Structure and Properties of Molybdenum Nitride and Molybdenum Carbonitride Films Prepared by Magnetron Sputtering, *Surf. Coat. Technol.*, 2019, **374**, p 725–735
27. C. Dang, J. Li, Y. Wang, Y. Yang, Y. Wang, and J. Chen, Influence of Ag Contents on Structure and Tribological Properties of TiSiN-Ag Nanocomposite Coatings on Ti_6Al_4V, *Appl. Surf. Sci.*, 2017, **394**, p 613–624
28. Y.X. Wang and S. Zhang, Toward Hard Yet Tough Ceramic Coatings, *Surf. Coat. Technol.*, 2014, **258**, p 1–16
29. A. Erdemir, A Crystal Chemical Approach to the Formulation of Self-Lubricating Nanocomposite Coatings, *Surf. Coat. Technol.*, 2005, **200**, p 1792–1796